CIRCULAR-APERTURE DIPOLE AND QUARDUPOLE MAGNETS: SHAPE, FIELD, ENERGY STORAGE, BODY-FORCES AND IRON SHIELD

by

Y. Iwasa and R.J. Weggel

Francis Bitter National Magnet Laboratory,*
Massachusetts Institute of Technology
Cambridge, Massachusetts 02139

Abstract

We have extended the work of Beth[1] and of Asner[2] to the design of circular-aperture dipoles and quadrupoles of arbitarily great winding depth. The i.d., o.d., and bounding angles of each annular wedge of current are chosen to best make the field multipolar outside as well as inside the system. This allows the use of a high-permeability shell to enhance the central field and reduce the fringing field without degrading the central homogeneity. We also present formulas for the field and magnetic energy storage, the magnetic body forces, and the thickness of iron needed to avoid saturation.

1. Introduction

The multipole magnets, particularly dipole and quadrupole, constitute a most important class of magnets. A majority of superconducting magnets, particularly those of the immediate future, are of this class: dipoles and quadrupoles in accelerators, and dipoles in MHD generators and superconducting alternators and related machines.

The field generated by these magnets ideally is identical in all planes perpendicular to the main axis; i.e. the field ideally is two-dimensional, and is always first approximated as such. Though not restricted to any particular shape, the aperture of these magnets is usually circular or elliptical, or, only occasionally, rectangular. We discuss here only the circular-aperture case, neglecting end effects but including the effects of an iron shield.

11. Dipoles

For circular-aperture dipoles with current distributions bounded between an i.d. of $2a_1$ and an o.d. of $2b_1$, such as those shown in Figs. 1 and 2, the magnetic field can be expressed as a sum of the fundamental and a power series of non-vanishing harmonics, beginning with $n=n^*$. Thus, for $r<a_1$:

$$\frac{H_{r,\theta}}{H_o} = D_1(K,C_1)\begin{Bmatrix}\sin\theta\\ \cos\theta\end{Bmatrix} + \sum_{n=n^*}^{\infty} D_n(K,n,C_1)\left(\frac{r}{a_1}\right)^{2n-2}\begin{Bmatrix}\sin(2n-1)\theta\\ \cos(2n-1)\theta\end{Bmatrix}, \quad (1)$$

and for $r>b_1$:

$$\frac{\tilde{H}_{r,\theta}}{H_o} = \tilde{D}_1(K,C_1)\left(\frac{b_1}{r}\right)^2\begin{Bmatrix}\sin\theta\\ \cos\theta\end{Bmatrix} + \sum_{n=n^*}^{\infty} \tilde{D}_n(K,n,C_1)\left(\frac{b_1}{r}\right)^{2n-2}\begin{Bmatrix}\sin(2n-1)\theta\\ \cos(2n-1)\theta\end{Bmatrix}, \quad (2)$$

where $C_1=b_1/a_1$, K is the number of current blocks in each quadrant, and the upper of the bracketed terms gives the r- component while the lower terms give the θ- component of the field. The normalizing field H_o, expressed in oersteds, is given by:

$$H_o = 0.4\pi a_1 (C_1-1)\, j_1, \quad (3)$$

with a_1 in cm and j_1, the current density in the first block, in A/cm^2.

For a dipole the ideal current distribution, the one for which only the fundamental component results, is cos θ. In practice, current-carrying blocks, within each of which the current density is uniform, are placed around the aperture to approximate the ideal current distribution. Two schemes are considered here. In the first, shown in Fig. 1, the current density differs from one block to the next, the winding thicknesses being identical; in the other, shown in Fig. 2, the winding thickness differs from one block to the next, the current densities being identical.

*Supported by the National Science Foundation.

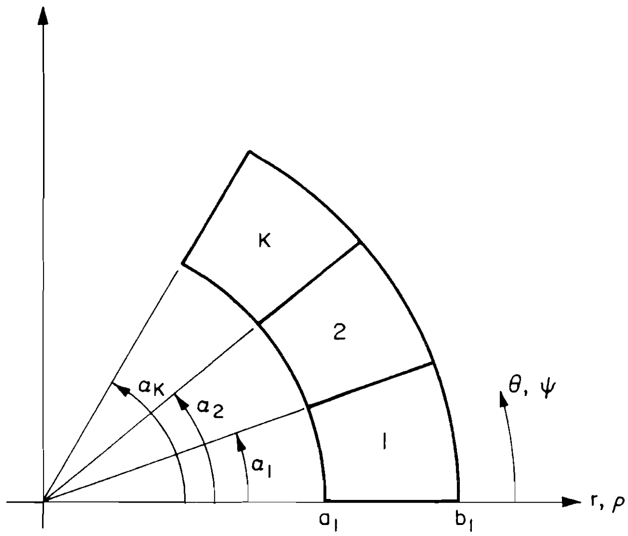

Fig. 1. Current-block arrangement for the first quadrant of the constant-winding-thickness dipole.

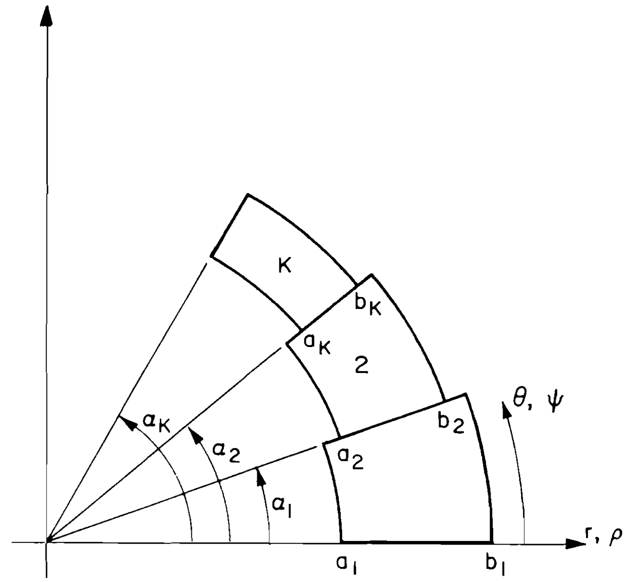

Fig. 2. Current-block arrangement for the first quadrant of the variable-winding-thickness dipole.

TABLE 1

PARAMETERS & COEFFICIENTS FOR CONSTANT-WINDING-THICKNESS DIPOLE

K=1	K=2	K=3	K=4
$\alpha_1=60^o$	$\alpha_1=36^o$; $\alpha_2=72^o$	$\alpha_1=25\ 5/7^o$; $\alpha_2=51\ 3/7^o$; $\alpha_3=77\ 1/7^o$	$\alpha_1=20^o$; $\alpha_2=40^o$; $\alpha_3=60^o$; $\alpha_4=80^o$
	$j_2/j_1=.6180$	$j_2/j_1=.8019$; $j_3/j_1=.4450$	$j_2/j_1=.8794$; $j_3/j_1=.6527$; $j_4/j_1=3473$

	K=1			K=2			K=3			K=4		
D_1		1.7320			1.6258			.7994			.7940	
C_1	$\tilde{D}_1$	$-D_3\times10$	$-\tilde{D}_3\times10$	$\tilde{D}_1$	$-D_5\times10$	$-\tilde{D}_5\times10$	$\tilde{D}_1$	$-D_7\times10^2$	$-\tilde{D}_7\times10^2$	$\tilde{D}_1$	$-D_9\times10^2$	$-\tilde{D}_9\times10^2$
1.0	1.7320	3.4640	3.4640	1.6258	1.8064	1.8064	1.5988	12.300	12.300	1.5880	9.3420	9.3420
1.2	1.4594	2.4320	2.1400	1.3698	.9302	.8528	1.3472	4.8380	4.6000	1.3380	2.9120	2.8580
1.4	1.2844	1.8348	1.5678	1.2056	.5840	.5606	1.1856	2.7260	2.8560	1.1776	1.5470	1.7180
1.6	1.1638	1.4546	1.2706	1.0924	.4140	.4354	1.0742	1.8528	2.1840	1.0670	1.0370	1.3110
1.8	1.0764	1.2958	1.0952	1.0102	.3174	.3688	.9936	1.3954	1.8446	.9868	.7784	1.1062
2.0	1.0104	1.0104	.9820	.9484	.2560	.3282	.9326	1.1176	1.6398	.9264	.6228	.9834
2.2	.9590	.8718	.9036	.9002	.2142	.3010	.8854	.9316	1.5032	.8794	.5190	.9014
2.4	.9182	.7652	.8464	.8618	.1839	.2816	.8476	.7986	1.4056	.8418	.4448	.8428
2.6	.8848	.6806	.8032	.8306	.1611	.2608	.8168	.6986	1.3324	.8112	.3892	.7990
2.8	.8592	.6122	.7692	.8046	.1433	.2554	.7912	.6212	1.2754	.7860	.3460	.7646
3.0	.8340	.5560	.7420	.7828	.1290	.2464	.7698	.5590	1.2298	.7646	.3114	.7374

$$D_n(K,n,C_1)=\frac{(C_1^{3-2n}-1)}{(2n-1)\ (3-2n)\ (C_1-1)}\ \frac{1}{j_1}\sum_{k=1}^{K} j_k\left(\sin\ (2n-1)\ \alpha_k - \sin\ (2n-1)\ \alpha_{k-1}\right)$$

$$\tilde{D}_n(K,n,C_1)=\frac{(C_1^{2n+1}-1)}{C_1^{2n}\ (2n-1)\ (2n+1)\ (C_1-1)}\ \frac{1}{j_1}\sum_{k=1}^{K} j_k\left(\sin\ (2n-1)\ \alpha_k - \sin\ (2n-1)\ \alpha_{k-1}\right)$$

In the first scheme, a proper choice of the current density and location of K blocks in each quadrant can eliminate all harmonics from n=2 through n=2K. In the second scheme the highest harmonic which can be eliminated is n=3K/2, with K an even number.

2.1. Constant Winding Thickness

For this scheme, shown in Fig. 1, both j_k, the current density in the kth block and α_k (with α_o=0) have been solved by Beth.[1] D_1, D_n*, $\tilde{D}_1$, and $\tilde{D}_n$*, and j_k are shown in Table 1. The field within the winding is relatively simple. We consider the dominant term only:

$$\frac{H_{r,\theta}}{H_o} = \left[\left(\frac{b_1 - r}{b_1 - a_1}\right) D_1 \pm \left(\frac{r^3 - a_1^3}{b_1^3 - a_1^3}\right)\left(\frac{b_1}{r}\right)^2 \tilde{D}_1\right]\begin{Bmatrix}\sin\theta\\ \cos\theta\end{Bmatrix}. \qquad (4)$$

The maximum occurs at $r=a_1$.

2.2 Variable Winding Thickness

Often this mode of winding is more convenient and economical of superconductor, because it maintains the same current density throughout the winding. Other schemes which do this, such as those shown in Fig. 3, eliminate only half as many harmonics per block of current. We must eliminate unwanted harmonics in the region $r>b_1$ as well as in the region $r<a_1$, because, as we shall see later when discussing iron shielding, the field in region $r>b_1$ determines the harmonics of the induced field generated by the iron shield. a_k, b_k, α_k, D_1, D_n*, $\tilde{D}_1$, and $\tilde{D}_n$* are given in Table 2.

TABLE 2

PARAMETERS & COEFFICIENTS FOR VARIABLE-WINDING-THICKNESS DIPOLE

K=2

c_1	a_2/a_1	b_2/a_1	α_1(o)	α_2(o)	D_1	$\tilde{D}_1$	$-D_4\times10^2$	$-\tilde{D}_4\times10^2$
1.2	1.039	1.163	36	72	1.6276	1.3714	.5390	.4648
1.4	1.077	1.329	36	72	1.6346	1.2120	1.1606	.9296
1.6	1.113	1.499	36	72	1.6436	1.1038	1.5290	1.1884
1.8	1.145	1.671	36	72	1.6530	1.0262	1.7004	1.3160
2.0	1.175	1.845	36	72	1.6624	.9680	1.7530	1.3722
2.2	1.202	2.021	36	72	1.6716	.9228	1.7398	1.3906
2.4	1.226	2.199	36	72	1.6800	.8870	1.6920	1.3890
2.6	1.248	2.377	36	72	1.6880	.8576	1.6276	1.3774
2.8	1.268	2.556	36	72	1.6954	.8332	1.5566	1.3610
3.0	1.286	2.735	36	72	1.7020	.8128	1.4846	1.3426

K=4

c_1	a_2/a_1	b_2/a_1	a_3/a_1	b_3/a_1	a_4/a_1	b_4/a_1	α_1(o)	α_2(o)	α_3(o)	α_4(o)	D_1	$\tilde{D}_1$	$-D_7\times10^3$	$-\tilde{D}_7\times10^4$
1.2	1.012	1.189	1.035	1.167	1.066	1.136	19.98	39.97	59.98	79.99	1.5908	1.3404	.159	.153
1.4	1.024	1.378	1.069	1.336	1.133	1.277	19.92	39.87	59.87	79.94	1.5996	1.1858	.743	.474
1.6	1.034	1.569	1.102	1.508	1.199	1.420	19.93	39.94	60.04	80.07	1.6104	1.0812	1.440	.403
1.8	1.043	1.762	1.130	1.684	1.261	1.567	19.82	39.75	59.85	79.98	1.6216	1.0060	1.909	.203
2.0	1.050	1.954	1.156	1.861	1.320	1.718	19.73	39.62	59.73	79.95	1.6328	.9498	2.010	1.070
2.2	1.057	2.148	1.179	2.040	1.375	1.871	19.64	39.49	59.63	79.92	1.6434	.9060	2.086	2.022
2.4	1.062	2.341	1.199	2.219	1.427	2.026	19.57	39.38	59.55	79.91	1.6534	.8712	2.086	2.956
2.6	1.067	2.535	1.218	2.400	1.477	2.182	19.50	39.29	59.49	79.91	1.6630	.8428	2.046	3.824
2.8	1.071	2.729	1.234	2.581	1.524	2.339	19.44	39.21	59.46	79.94	1.6716	.8192	1.988	4.616
3.0	1.075	2.924	1.249	2.762	1.568	2.497	19.40	39.15	55.45	79.99	1.6798	.7994	1.924	5.340

$$D_n(K,n,C_1) = \frac{1}{(2n-1)\ (3-2n)\ (C_1-1)} \sum_{k=1}^{K} \left[\left(\frac{b_k}{a_1}\right)^{3-2n} - \left(\frac{a_k}{a_1}\right)^{3-2n}\right]\left\{\sin(2n-1)\alpha_k - \sin(2n-1)\ \alpha_{k-1}\right\}$$

$$\tilde{D}_n(K,n,C_1) = \frac{1}{C_1^{2n}\ (2n-1)\ (2n+1)\ (C_1-1)} \sum_{k=1}^{K} \left[\left(\frac{b_k}{a_1}\right)^{2n+1} - \left(\frac{a_k}{a_1}\right)^{2n+1}\right]\left\{\sin(2n-1)\alpha_k - \sin(2n-1)\alpha_{k-1}\right\}$$

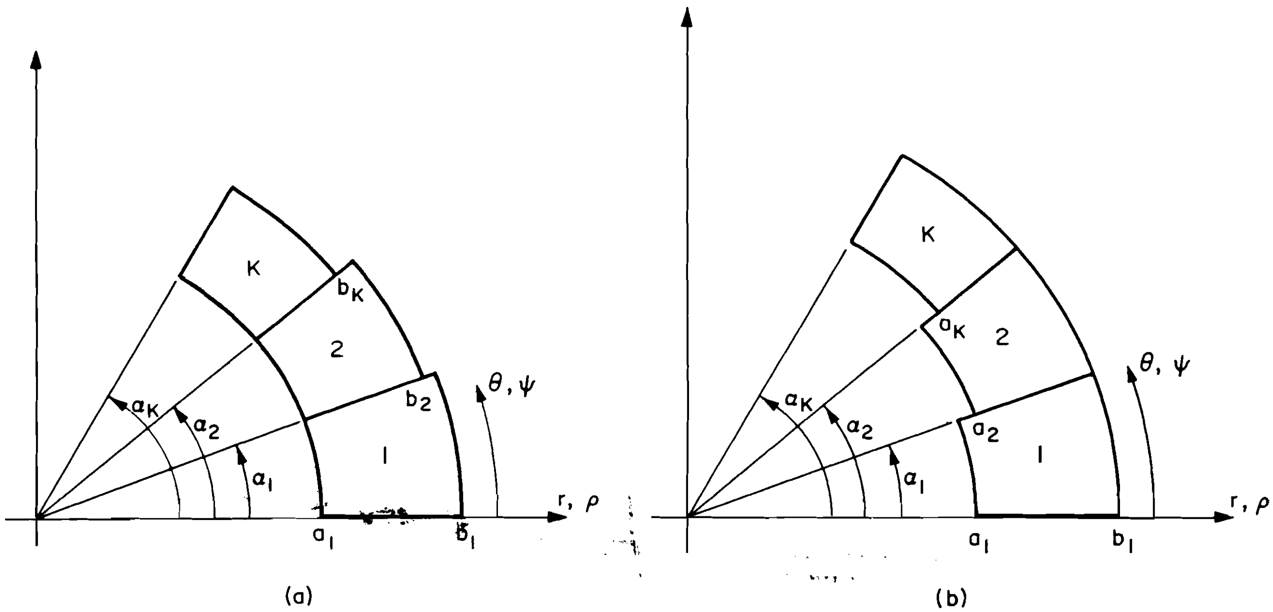

Fig. 3. Two other possible current-block arrangements for the first quadrant of the dipole.

111. Quadrupoles

A procedure entirely similar to that used for the dipole is applicable to the quadrupoles shown in Figs. 4 and 5. Thus, for $r<a_1$:

$$\frac{H_{r,\theta}}{H_o} = \pm\, Q_1(K,C_1)\left(\frac{r}{a_1}\right)\begin{Bmatrix}\cos 2\theta\\ \sin 2\theta\end{Bmatrix} \pm \sum_{n=n^*}^{\infty} Q_n(K,n,C_1)\left(\frac{r}{a_1}\right)^{4n-3}\begin{Bmatrix}\cos\,(4n-2)\theta\\ \sin\,(4n-2)\theta\end{Bmatrix}, \qquad (5)$$

and for $r>b_1$:

$$\frac{\tilde{H}_{r,\theta}}{H_o} = +\,\tilde{Q}_1(K,C_1)\left(\frac{b_1}{r}\right)^3\begin{Bmatrix}\cos 2\theta\\ \sin 2\theta\end{Bmatrix} + \sum_{n=n^*}^{\infty} \tilde{Q}_n(K,n,C_1)\left(\frac{b_1}{r}\right)^{4n-1}\begin{Bmatrix}\cos(4n-2)\theta\\ \sin(4n-2)\theta\end{Bmatrix}. \qquad (6)$$

In the quadrupole magnet, one is interested also in the field gradient for $r<a_1$, the gradients along two important radii, $\Theta=0$ and $\Theta=\pi/4$, being:

$$g_r \equiv \left[\frac{\partial H_r}{\partial r}\right]_{\Theta=0} = -\frac{H_o}{a_1}\left[Q_1(K,C_1) + \sum_{n=n^*}^{\infty} Q_n(K,n,C_1)\ (4n-3)\left(\frac{r}{a_1}\right)^{4n-4}\right], \qquad (7)$$

$$g_\Theta \equiv \left[\frac{\partial H\Theta}{\partial r}\right]_{\Theta=\pi/4} = \frac{H_o}{a_1}\left[Q_1(K,C_1) + \sum_{n=n^*}^{\infty} (-1)^{n+1} Q_n(K,n,C_1)\ (4n-3)\left(\frac{r}{a_1}\right)^{4n-4}\right]. \qquad (8)$$

3.1 Constant Winding Thickness

For this scheme, shown in Fig. 4, the required value of each α_k, now measured from the 45 degree line, is one half that for the dipole of constant winding thickness; each j_k is unchanged. Q_1, Q_{n^*}, $\tilde{Q}_1$ and $\tilde{Q}_{n^*}$ are tabulated in Table 3. The dominant term of the magnetic field within the winding is:

$$\frac{H_{r,\theta}}{H_o} = \pm\, Q_1\left(\frac{\ell n\ b_1/r}{\ell n\ C_1}\right)\left(\frac{r}{a_1}\right)\begin{Bmatrix}\cos 2\ \theta\\ \sin 2\ \theta\end{Bmatrix} + \tilde{Q}_1\left(\frac{r^4-a_1^4}{b_1^4-a_1^4}\right)\left(\frac{b_1}{r}\right)^3\begin{Bmatrix}\cos 2\ \theta\\ \sin 2\ \theta\end{Bmatrix}, \qquad (9)$$

which is maximum for $r>a_1$. The location and value of this maximum is included in Table 3.

3.2 Variable Winding Thickness

For this scheme, shown in Fig. 5, appropriate values of a_k, b_k, and α_k are tabulated together with Q_1, Q_{n^*}, $\tilde{Q}_1$, and $\tilde{Q}_{n^*}$ in Table 4.

IV. Iron Shielding

It is usually desirable to minimize the intense fields immediately outside multipole magnets. This can be done either with reverse

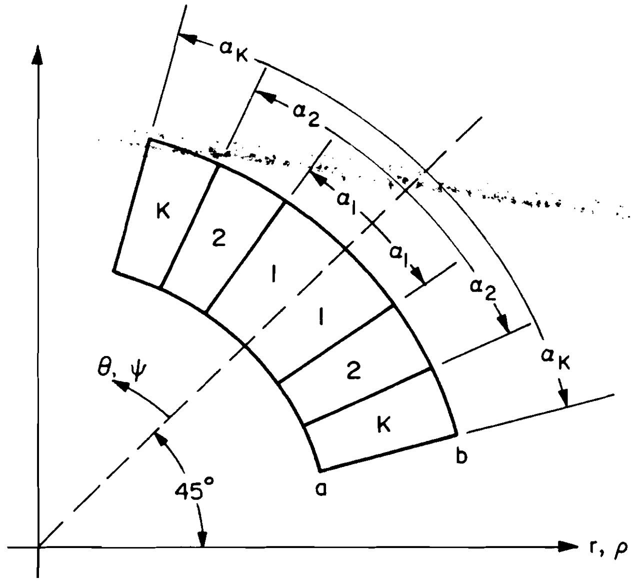

Fig. 4. Current-block arrangement for the first quadrant of the constant-winding-thickness quadrupole.

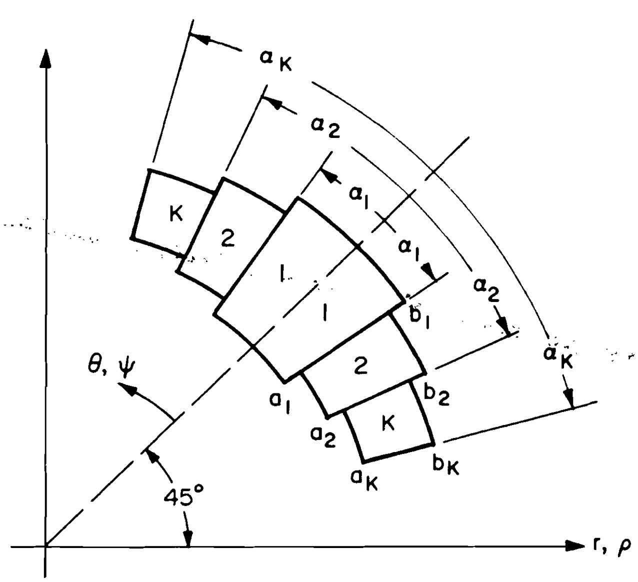

Fig. 5. Current-block arrangement for the first quadrant of the variable-winding-thickness quadrupole.

windings, which decrease the useful field, or with an iron shield, which increases it. The iron shield also makes the internal field less sensitive to its external environment. Here we discuss iron-shields for circular-aperture multipoles in general, and derive expressions for the total magnetic field for the circular-aperture dipoles and quadrupoles analyzed above. We assume the magnetic permeability of the iron to be infinite and calculate the thickness of the shield necessary to make the assumption valid.[3]

Given a circular-field winding confined between $r=a_1$ and $r=b_1>a_1$, let the resultant magnetic fields be $H(r/a_1, \Theta)$ for $r>b_1$. Suppose we add a circular-aperture iron shield of inside radius $b_s>b_1$. Since the permeability is assumed infinite, the tangential component of the total field must vanish at $r=b_s$. That is:

$$\tilde{H}_\Theta (b_1/b_s, \Theta) + H_{s\Theta} (r=b_s, \Theta) = 0, \qquad (10)$$

where $H_{s\Theta}(r,\Theta)$ is the Θ component of the additional magnetic field due to the presence of the shield, derivable from a potential. Since $H(r/a_1, \Theta)$ and $\tilde{H}(b_1/r, \Theta)$ are themselves derived from potentials, it is reasonable to assume $H_s(r, \Theta)$ is of the form $H(r/a_1, \Theta)$ or $\tilde{H}(b_1/r, \Theta)$. Because $H_s(r,\Theta)$ must be finite for $r<b_s$, it follows $H_s(r,\Theta)$ is of the form $H(r/a_1,\Theta)$ with a_1 replaced by b_s. Thus:

$$H_s(r,\Theta) = C_s\, H(r/b_s, \Theta), \qquad (11)$$

where C_s is a constant determined solely by the boundary condition given by Eq. 10. It is clear, therefore, that any harmonic present in $\tilde{H}(b_1/r,\Theta)$ will appear in $H_s(r,\Theta)$, indicating the importance of eliminating harmonics for $r>b_1$ as well as $r<a_1$.

4.1. Dipoles

Applying Eqs. 10 and 11, we have expressions for the r and Θ components of $H_s(r,\Theta)$ as follows:

$$\left(\frac{H_s}{H_o}\right)_{r,\Theta} = \tilde{D}_1 \left(\frac{b_1}{b_s}\right)^2 \begin{Bmatrix}\sin\Theta\\ \cos\Theta\end{Bmatrix} + \sum_{n=n^*}^{\infty} \tilde{D}_n \left(\frac{b_1}{b_s}\right)^{2n} \left(\frac{r}{b_s}\right)^{2n-2} \begin{Bmatrix}\sin(2n-1)\Theta\\ \cos(2n-1)\Theta\end{Bmatrix}. \qquad (12)$$

Thus expressions for the r and Θ components of the total field become:

$$\left(\frac{H_T}{H_o}\right)_{r,\Theta} = \left[D_1 + \tilde{D}_1 \left(\frac{b_1}{b_s}\right)^2\right] \begin{Bmatrix}\sin\Theta\\ \cos\Theta\end{Bmatrix} + \sum_{n=n^*}^{\infty} \left[D_n + \tilde{D}_n \frac{(a_1 b_1)^{2n}}{b_s^{4n}} \left(\frac{b_s}{a_1}\right)^2\right] \left(\frac{r}{a_1}\right)^{2n-2} \begin{Bmatrix}\sin(2n-1)\Theta\\ \cos(2n-1)\Theta\end{Bmatrix}, \qquad (13)$$

for $r<a_1$ and:

$$\left(\frac{\tilde{H}_T}{H_o}\right)_{r,\Theta} = \pm \tilde{D}_1 \left[\left(\frac{b_1}{r}\right)^2 \pm \left(\frac{b_1}{b_s}\right)^2\right] \begin{Bmatrix}\sin\Theta\\ \cos\Theta\end{Bmatrix} + \sum_{n=n^*}^{\infty} \tilde{D}_n \left[\left(\frac{b_1}{r}\right)^{2n} \pm \frac{(a_1 b_1)^{2n}}{b_s^{4n}} \left(\frac{b_s}{a_1}\right)^2 \left(\frac{r}{a_1}\right)^{2n-2}\right] \begin{Bmatrix}\sin(2n-1)\Theta\\ \cos(2n-1)\Theta\end{Bmatrix} \qquad (14)$$

for $b_1 < r \leq b_s$.

TABLE 3

PARAMETERS & COEFFICIENTS FOR CONSTANT-WINDING-THICKNESS QUARDUPOLE

K=1

$\alpha_1=30^\circ$

$j_1/j_1=1$

c_1	Q_1	$\tilde{Q}_1$	Q_3x10	$\tilde{Q}_3$x10	$(r/a_1)^*$	$(H/H_c)^+$
1.0	1.7320	1.7320	3.4640	3.4640	1.00	1.000
1.2	1.5790	1.3452	1.6616	1.5378	1.	1.
1.4	1.4570	1.1210	1.0092	.9926	1.	1.
1.6	1.3568	.9786	.7048	.7670	1.	1.
1.8	1.2726	.8814	.5364	.6490	1.07	1.005
2.0	1.2006	.8120	.4314	.5772	1.14	1.019
2.2	1.1380	.7600	.3602	.5292	1.20	1.035
2.4	1.0832	.7200	.3090	.4948	1.26	1.053
2.6	1.0342	.6882	.2706	.4690	1.33	1.071
2.8	.9908	.6626	.2405	.4490	1.39	1.090
3.0	.9514	.6416	.2164	.4330	1.46	1.110

K=2

$\alpha_1=18^\circ$; $\alpha_2=36^\circ$

$j_2/j_1=.6180$

c_1	Q_1	$\tilde{Q}_1$	Q_5x10^2	$\tilde{Q}_5$x10^2	$(r/a_1)^*$	$(H/H_c)^+$
1.0	1.6258	1.6258	13.500	13.500	1.00	1.000
1.2	1.4820	1.2626	5.3400	5.2780	1.	1.
1.4	1.3676	1.0522	2.8100	3.1580	1.06	1.013
1.6	1.2736	.9184	1.8806	2.4080	1.12	1.034
1.8	1.1946	.8274	1.4112	2.0320	1.17	1.054
2.0	1.1270	.7620	1.1290	1.8064	1.23	1.075
2.2	1.0682	.7134	.9408	1.6560	1.29	1.096
2.4	1.0166	.6758	.8064	1.5484	1.35	1.117
2.6	.9710	.6460	.7056	1.4678	1.14	1.138
2.8	.9300	.6220	.6272	1.4050	1.48	1.159
3.0	.8930	.6022	.5646	1.3548	1.55	1.180

K=3

$\alpha_1=12\ 6/7^\circ$; $\alpha_2=25\ 5/7^\circ$; $\alpha_3=38\ 4/7^\circ$

$j_2/j_1=.8019$; $j_3/j_1=.4450$

c_1	Q_1	$\tilde{Q}_1$	Q_7x10^2	$\tilde{Q}_7$x10^2	$(r/a_1)^*$	$(H/H_c)^+$
1.0	1.5988	1.5988	12.300	12.300	1.00	1.000
1.2	1.4576	1.2416	2.5300	2.6200	1.03	1.007
1.4	1.3450	1.0348	1.2808	1.5372	1.09	1.029
1.6	1.2524	.9032	.8540	1.1714	1.14	1.051
1.8	1.1748	.8136	.6406	.9882	1.19	1.072
2.0	1.1082	.7494	.5124	.8784	1.25	1.094
2.2	1.0506	.7016	.4270	.8052	1.31	1.115
2.4	.9998	.6646	.3660	.7530	1.37	1.136
2.6	.9548	.6354	.3202	.7138	1.43	1.158
2.8	.9146	.6117	.2846	.6832	1.50	1.179
3.0	.8782	.5922	.2562	.6588	1.57	1.201

K=4

$\alpha_1=10^\circ$; $\alpha_2=20^\circ$; $\alpha_3=30^\circ$; $\alpha_4=40^\circ$

$j_2/j_1=.8794$; $j_3/j_1=.6527$; $j_4/j_1=.3473$

c_1	Q_1	$\tilde{Q}_1$	Q_9x10^2	$\tilde{Q}_9$x10^2	$(r/a_1)^*$	$(H/H_c)^+$
1.0	1.5880	1.5880	9.3400	9.3400	1.00	1.000
1.2	1.4476	1.2334	1.4554	1.5558	1.04	1.013
1.4	1.3358	1.0278	.7298	.9082	1.09	1.036
1.6	1.2440	.8972	.4866	.6920	1.14	1.058
1.8	1.1668	.8082	.3650	.5838	1.20	1.080
2.0	1.1008	.7444	.2920	.5190	1.25	1.101
2.2	1.0434	.6968	.2432	.4758	1.31	1.123
2.4	.9930	.6600	.2086	.4448	1.38	1.145
2.6	.9484	.6310	.1825	.4216	1.44	1.166
2.8	.9084	.6076	.1622	.4036	1.51	1.188
3.0	.8724	.5882	.1460	.3892	1.58	1.210

$H_c=H_oQ_1$

* Location of Maximum Field

\+ Maximum Field

$$Q_1(K,C_1)=\frac{1}{(C_1-1)}\ \ln C_1\ \frac{1}{j_1}\sum_{k=1}^{K} j_k\ (\sin 2\alpha_k-\sin 2\alpha_{k-1})$$

$$Q_{n>1}\ (K,n,C_1)=\frac{(-1)^n\ (C_1^{\ 4n-4}-1)}{(C_1-1)\ (2n-1)\ (4n-4)\ C_1^{\ 4n-4}}\ \frac{1}{j_1}\sum_{k=1}^{K} j_k\left(\sin(4n-2)\alpha_k-\sin\ (4n-2)\alpha_{k-1}\right)$$

$$\tilde{Q}_n(K,n,C_1)=\frac{(-1)^n\ (C_1^{\ 4n}-1)}{(2n-1)\ (4n)\ (C_1-1)\ C^{4n-1}}\ \frac{1}{j_1}\sum_{k=1}^{K} j_k\left(\sin(4n-2)\ \alpha_k-\sin\ (4n-2)\alpha_{k-1}\right)$$

4.2. Quadrupoles

Similarly for the quadrupoles, the total magnetic fields are for $r<a_1$:

$$\left(\frac{H_T}{H_o}\right)_{r,\theta} = \pm\left[Q_1 + \tilde{Q}_1 \frac{a_1 b_1^3}{b_s^4}\right]\left(\frac{r}{a_1}\right)\begin{Bmatrix}\cos 2\theta \\ \sin 2\theta\end{Bmatrix} \pm \sum_{n=n*}^{\infty}\left[Q_n + \tilde{Q}_n \frac{(a_1 b_1)^{4n} b_s^4}{b_s^{8n}\,(b_1 a_1)^3}\right]\left(\frac{r}{a_1}\right)^{4n-3}\begin{Bmatrix}\cos(4n-2\theta \\ \sin(4n-2\theta\end{Bmatrix}, \quad (15)$$

and for $b_1 < r < b_s$:

$$\left(\frac{\tilde{H}_T}{H_o}\right)_{r,\theta} = +\tilde{Q}_1\left[\left(\frac{b_1}{r}\right)^3 \pm \frac{a_1 b_1^3}{b_s^4}\left(\frac{r}{a_1}\right)\right]\begin{Bmatrix}\cos 2\theta \\ \sin 2\theta\end{Bmatrix} + \sum_{n=n*}^{\infty}\tilde{Q}_n\left[\left(\frac{b_1}{r}\right)^{4n-1} + \frac{(a_1 b_1)^{4n} b_s^4}{b_s^{8n}\,(b_1 a_1^3)}\left(\frac{r}{a_1}\right)^{4n-3}\right]\begin{Bmatrix}\cos(4n-2\theta \\ \sin(4n-2\theta\end{Bmatrix}. \quad (16)$$

TABLE 4

PARAMETERS & COEFFICIENTS FOR VARIABLE-WINDING-THICKNESS QUADRUPOLE

K=2

c_1	a_2/a_1	b_2/a_1	$\alpha_1(^o)$	$\alpha_2(^o)$	Q_1	$\tilde{Q}_1$	$Q_4 x10^2$	$-\tilde{Q}_4 x10^2$
1.2	1.037	1.164	18	36	1.4918	1.2708	1.1863	1.0570
1.4	1.067	1.337	18	36	1.3975	1.0743	1.6537	1.4591
1.6	1.088	1.516	18	36	1.3223	.9508	1.5880	1.4511
1.8	1.102	1.700	18	36	1.2576	.8659	1.4024	1.3529
2.0	1.110	1.886	18	36	1.1998	.8037	1.2195	1.2528
2.2	1.116	2.073	18	36	1.1476	.7563	1.0650	1.1691
2.4	1.119	2.261	18	36	1.1000	.7190	.9389	1.1023
2.6	1.121	2.449	18	36	1.0567	.6891	.8363	1.0492
2.8	1.123	2.637	18	36	1.0170	.6646	.7523	1.0064
3.0	1.124	2.825	18	36	.9805	.6443	.6826	.9716

K=4

c_1	a_2/a_1	b_2/a_1	a_3/a_1	b_3/a_1	a_4/a_1	b_4/a_1	$\alpha_1(^o)$	$\alpha_2(^o)$	$\alpha_3(^o)$	$\alpha_4(^o)$	Q_1	$\tilde{Q}_1$	$-Q_7 x10^3$	$\tilde{Q}_7 x10^4$
1.2	1.011	1.189	1.034	1.168	1.065	1.138	9.97	19.95	29.94	39.97	1.4601	1.2437	.6838	2.6894
1.4	1.020	1.381	1.060	1.343	1.123	1.285	9.89	19.83	29.83	39.91	1.3719	1.0541	1.5177	5.0271
1.6	1.025	1.576	1.078	1.525	1.166	1.444	9.78	19.63	29.59	39.76	1.3019	.9350	1.5721	4.1790
1.8	1.028	1.771	1.089	1.711	1.196	1.612	9.70	19.47	29.41	39.63	1.2421	.8533	1.4064	2.9763
2.0	1.030	1.967	1.096	1.898	1.216	1.785	9.64	19.37	29.28	39.54	1.1890	.7937	1.2309	2.1341
2.2	1.031	2.164	1.101	2.087	1.229	1.961	9.60	19.30	29.21	39.49	1.1407	.7482	1.0819	1.5910
2.4	1.032	2.360	1.104	2.276	1.238	2.138	9.58	19.26	29.17	39.46	1.0964	.7124	.9597	1.2340
2.6	1.033	2.557	1.106	2.466	1.244	2.316	9.57	19.24	29.14	39.44	1.0556	.6835	.8592	.9921
2.8	1.033	2.753	1.108	2.655	1.248	2.494	9.56	19.22	29.12	39.43	1.0179	.6598	.7760	.8235
3.0	1.033	2.950	1.109	2.845	1.251	2.672	9.55	19.21	29.11	39.42	.9831	.6399	.7064	.7033

$$Q_1(K,C_1) = \frac{2}{(C_1-1)}\ \frac{1}{j_1}\sum_{k=1}^{K}\ln\left(\frac{b_k}{a_k}\right)\left(\sin 2\alpha_k - \sin 2\alpha_k{-}1\right)$$

$$Q_{n>1}(K,n,C_1) = \frac{(-1)^n}{(2n-1)(2n-2)}\ \frac{1}{j_1}\sum_{k=1}^{K}\left[\left(\frac{b_k}{a_1}\right)^{4-4n} - \left(\frac{a_k}{a_1}\right)^{4-4n}\right]\left(\sin(4n-2)\alpha_k - \sin(4n-2)\alpha_k{-}1\right)$$

$$\tilde{Q}_n(K,n,C_1) = \frac{(-1)^{n+1}}{(C_1-1)\ (2n-1)\ (2n)\ C_1^{4n-1}}\ \frac{1}{j_1}\sum_{k=1}^{k}\left[\left(\frac{b_k}{a_1}\right)^{4n} - \left(\frac{a_k}{a_1}\right)^{4n}\right]\left(\sin(4n-2)\alpha_k - \sin(4n-2)\alpha_{k-1}\right)$$

4.3 Thickness of Iron Cladding

The magnetic field within an iron shield should not exceed 16,000 gauss or so. Its thickness, therefore, should satisfy the relationship:

$$16{,}000\ W \geq b_s \int_0^{\pi/2} [\,H_T(r{=}b_s)\,]_r \, d\Theta, \qquad (17)$$

for the dipole and

$$16{,}000\ W \geq b_s \int_0^{\pi/4} [\,H_T(r{=}b_s)\,]_r \, d\Theta, \qquad (18)$$

for the quadrupole. Combining Eqs. 14 and 17 for the dipole:

$$\frac{W}{b_s} \geq 2\, \frac{H_o \tilde{D}_1}{16{,}000} \left(\frac{b_1}{b_s}\right)^2, \qquad (19)$$

and Eqs. 23 and 25 for the quadrupole:

$$\frac{W}{b_s} \geq \frac{H_o \tilde{Q}_1}{16{,}000} \left(\frac{b_1}{b_s}\right)^3. \qquad (20)$$

V. Energy Storage

We give here approximate expressions for the magnetic energy storage for circular-aperture, iron-shielded dipoles and quadrupoles of constant winding thickness.

5.1. Dipoles

The magnetic energy per unit length, E_M(J/m) is:

$$\frac{E_M}{E_o} = 1 + \frac{(C_1^2+C_1+1)^2}{9\,C_1^2} \left\{ 1 + 2\,(b_1/b_s)^2 \right\},$$

$$\equiv e_D\,(C_1,\ b_1/b_s)\,, \qquad (21)$$

where

$$E_o = 0.8\text{x}10^{-6}\,((C_1-1)\,a_1^2 j_1 D_1)^2\ \text{J/m}. \qquad (22)$$

We have neglected the magnetic energy stored in the iron shield; since the thickness of the shield is chosen to keep the iron from saturating, the energy stored in the shield is indeed small. For the case with no shield, the (b_1/b_s) term becomes zero. $e_D(c_1, b_1/b_s)$ is given in Fig. 6.

5.2. Quadrupoles

Similarly, the stored energy for a quadrupole of constant winding thickness is:

$$\frac{E_M}{E_o} = \left[\left\{ \frac{C_1^4-1}{4(\ln C_1)^2} - \frac{1}{\ln C_1} \right\} + \frac{(C_1^4-1)^2}{8C_1^4(\ln C_1)^2} \left(\frac{b_1}{b_s}\right)^4 \right],$$

$$\equiv e_Q\,(C_1,\ b_1/b_s)\,, \qquad (23)$$

where

$$E_o = 0.4\text{x}10^{-6}\,((C_1-1)\,a_1^2 j_1 D_1)^2\ \text{J/m}. \qquad (24)$$

$e_Q(c_1, b_1/b_s)$ is plotted in Fig. 7.

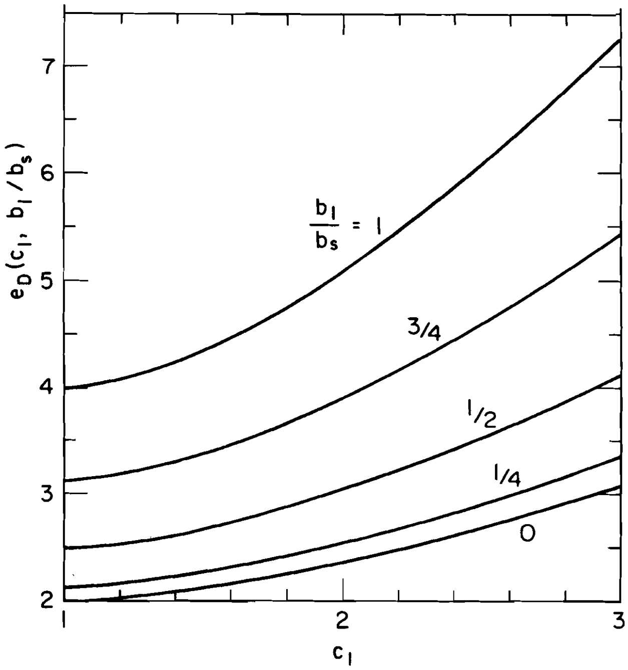

Fig. 6. The geometry-dependent factor e_D which gives the energy storage of a constant-winding-thickness dipole of type shown in Fig. 1.

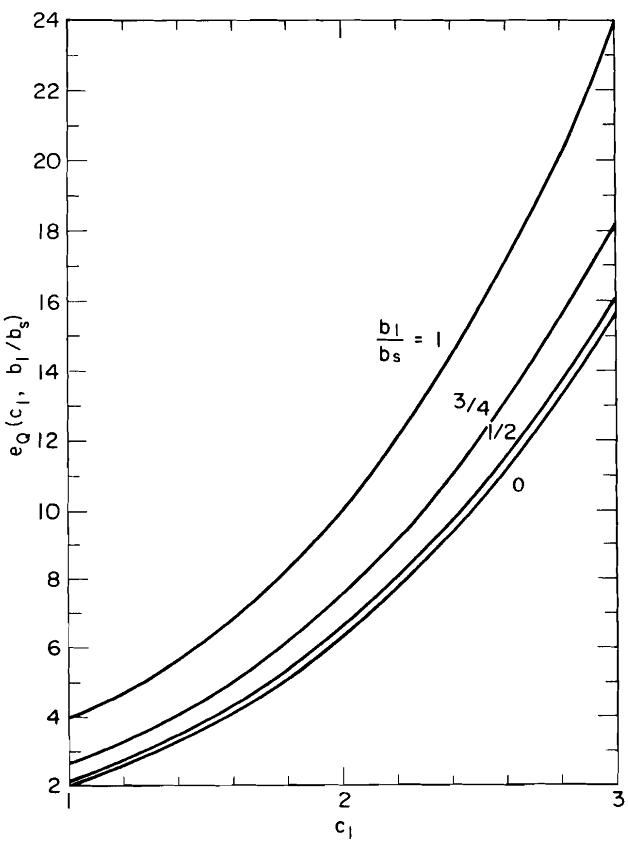

Fig. 7. The geometry-dependent factor e_Q which gives the energy storage of a constant-winding-thickness quadrupole of type shown in Fig. 4.

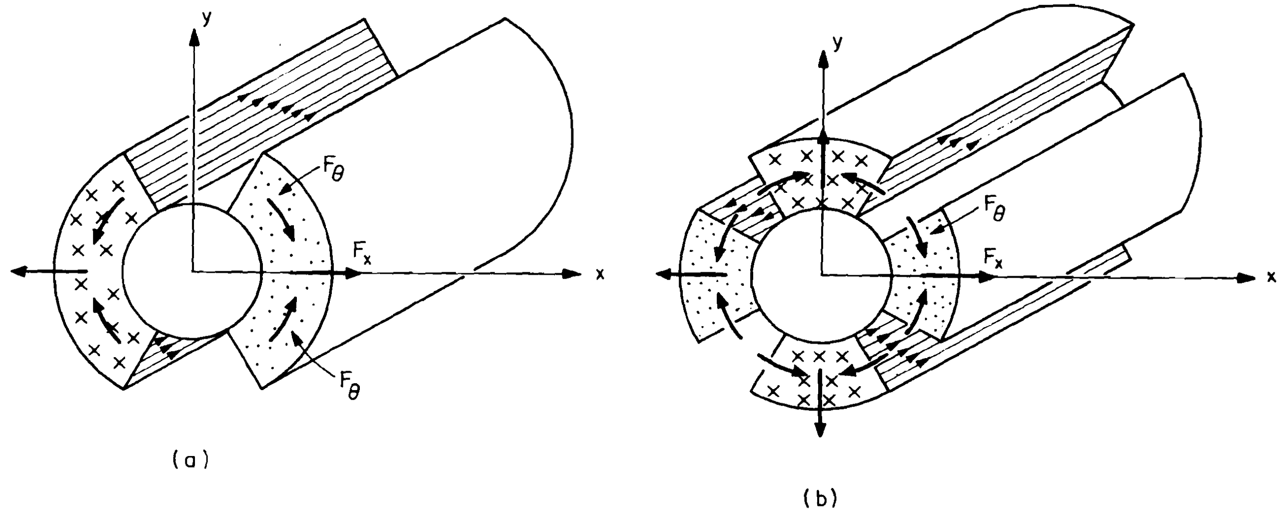

Fig. 8. Body-force distributions for: (a) Dipole and (b) Quadrupole.

VI. Magnetic Body Forces

We examine the magnetic body forces resulting from the Lorentz interaction in constant-winding-thickness dipoles and quadrupoles with circular-aperture iron shields. Results for magnets of variable winding thickness should be similar. The body forces give a good indication, expecially in "thin coils", of the level of magnetic stresses within the winding.

6.1. Dipoles

The magnetic field within the winding of a dipole of constant winding thickness is given by Eq. 4. To this we must add the field contribution of the iron shielding, given by Eq. 12. The resulting total field (based on the dominant term only) is:

$$\frac{H_{r,\theta}}{H_o} = \left[\left(\frac{b_1 - r}{b_1 - a_1}\right) D_1 \pm \left(\frac{r^3 - a_1^3}{b_1^3 - a_1^3}\right)\left(\frac{b_1}{r}\right)^2 \tilde{D}_1 + \left(\frac{b_1}{b_s}\right)^2 \tilde{D}_1\right]\left\{\begin{matrix}\sin\theta\\ \cos\theta\end{matrix}\right\} \qquad (25)$$

The body forces in the dipole act as shown in Fig. 8a. We define two components of the body force, one in the x-direction, F_x, which tends to burst the magnet and the other in the direction, F_θ, which tends to crush it circumferentially. These forces, per unit length of magnet, are:

$$F_x = \int_{a_1}^{b_1} r dr \sum_{k=1}^{K} \int_{-\alpha_k}^{\alpha_k} d\theta \; j_k \; H_\theta \cos\theta \qquad (26)$$

$$F_\theta = \int_{a_1}^{b_1} r dr \sum_{k=1}^{K} \int_{o}^{\alpha_k} d\theta \; j_k \; H_r \; . \qquad (27)$$

Combining Eqs. 25,26, and 27 we obtain:

$$F_x = \left(\frac{10^{-4}}{9.8}\right) j_1 \, H_o \, D_1 \, a_1^2 \, f_{Dx} \, (C_1, K) \qquad (28)$$

$$F_\theta = \left(\frac{10^{-4}}{9.8}\right) j_1 \, H_o \, D_1 \, a_1^2 \, f_{D\theta} \, (C_1), \qquad (29)$$

where the forces are in kg/m; H_o, given by Eq. 3, is in oersted, j_1 is in A/cm^2, and a_1 is in cm. f_{Dx} depends on K, though only weakly, while $f_{D\theta}$ does not. Both are plotted as a function of C_1 and for several values of b_1/b_s in Fig. 9. Note that iron shielding greatly increases F_x.

6.2 Quadrupoles

An identical approach computes body forces in a quadrupole of constant winding thickness. The total field within the winding is:

$$\frac{H_{r,\theta}}{H_o} = \left[\pm Q_1\left(\frac{\ln b_1/r}{\ln C_1}\right)\frac{r}{a_1} + \tilde{Q}_1\left(\frac{r^4 - a_1^4}{b_1^4 - a_1^4}\right)\left(\frac{b_1}{r}\right)^3 \pm \tilde{Q}_1\left(\frac{a_1 b_1^3}{b_s^4}\right)\frac{r}{a_1}\right]\left\{\begin{matrix}\cos 2\theta\\ \sin 2\theta\end{matrix}\right\} \qquad (30)$$

The resulting body forces are shown in Fig. 8b. Again we decompose them into two components, x and Θ:

$$F_x = \frac{(10^{-4})}{9.8} j_1 H_o D_1 a_1^2 f_{Qx} (C_1, K) \quad (31)$$

$$F_\Theta = \frac{(10^{-4})}{9.8} j_1 H_o D_1 a_1^2 f_{QD} (C_1) \quad (32)$$

where the forces again are in kg/m. f_{Qx} and $f_{Q\Theta}$ are plotted in Fig. 10.

References

1. R. A. Beth, Proc. 1968 Summer Study on Superconducting Devices and Accelerators, A. G. Prodell, Ed. (Brookhaven National Laboratory, Upton, New York 1969), p. 843.
2. A. Asner, ibid., p. 866.
3. J. P. Blewett, ibid., p. 1042.

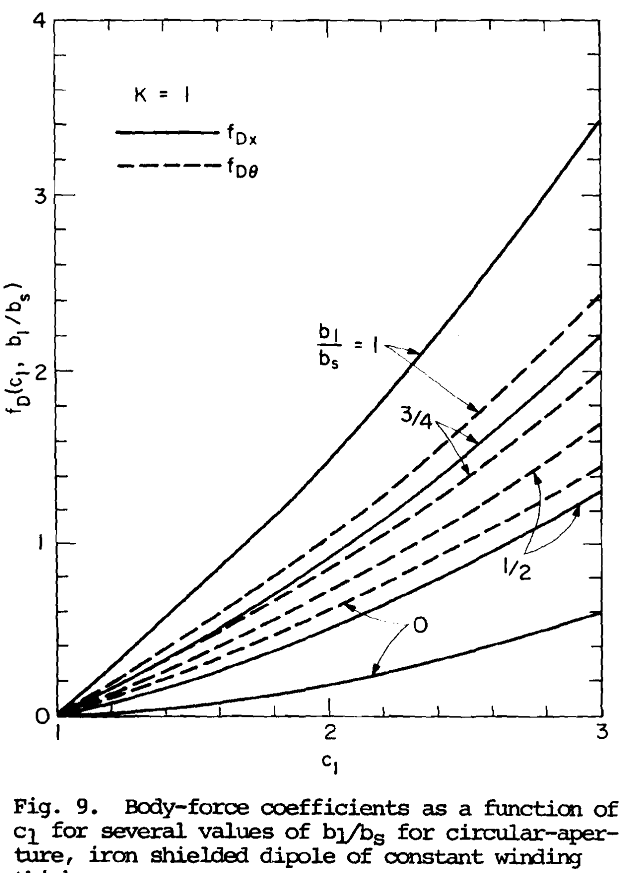

Fig. 9. Body-force coefficients as a function of c_1 for several values of b_1/b_s for circular-aperture, iron shielded dipole of constant winding thickness.

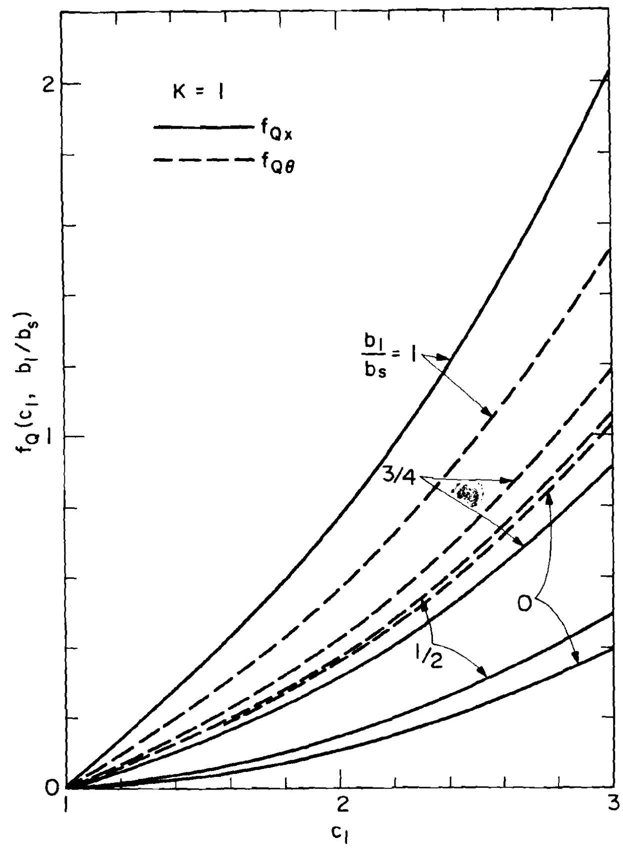

Fig. 10. Body-force coefficients as a function of c_1 for several values of b_1/b_s for circular-aperture, iron-shielded quadrupole of constant winding thickness.